^{18}F-FLT PET Does Not Discriminate Between Reactive and Metastatic Lymph Nodes in Primary Head and Neck Cancer Patients

Esther G.C. Troost[1], Wouter V. Vogel[2], Matthias A.W. Merkx[3], Piet J. Slootweg[4], Henri A.M. Marres[5], Wenny J.M. Peeters[1], Johan Bussink[1], Albert J. van der Kogel[1], Wim J.G. Oyen[2], and Johannes H.A.M. Kaanders[1]

[1]Department of Radiation Oncology, Radboud University Nijmegen Medical Centre, Nijmegen, The Netherlands; [2]Department of Nuclear Medicine, Radboud University Nijmegen Medical Centre, Nijmegen, The Netherlands; [3]Department of Oral and Maxillofacial Surgery, Radboud University Nijmegen Medical Centre, Nijmegen, The Netherlands; [4]Department of Pathology, Radboud University Nijmegen Medical Centre, Nijmegen, The Netherlands; and [5]Department of Otorhinolaryngology, Head and Neck Surgery, Radboud University Nijmegen Medical Centre, Nijmegen, The Netherlands

Repopulation of clonogenic tumor cells is inversely correlated with radiation treatment outcome in head and neck squamous cell carcinomas. A functional imaging tool to assess the proliferative activity of tumors could improve patient selection for treatment modifications and could be used for evaluation of early treatment response. The PET tracer 3′-deoxy-3′-^{18}F-fluorothymidine (^{18}F-FLT) can image tumor cell proliferation before and during radiotherapy, and it may provide biologic tumor information useful in radiotherapy planning. In the present study, the value of ^{18}F-FLT PET in determining the lymph node status in squamous cell carcinoma of the head and neck was assessed, with pathology as the gold standard. **Methods:** Ten patients with newly diagnosed stage II–IV squamous cell carcinoma of the head and neck underwent ^{18}F-FLT PET before surgical tumor resection with lymph node dissection. Emission ^{18}F-FLT PET and CT images of the head and neck were recorded and fused, and standardized uptake values (SUVs) were calculated. From all 18 ^{18}F-FLT PET-positive lymph node levels and from 8 ^{18}F-FLT PET-negative controls, paraffin-embedded lymph node sections were stained and analyzed for the endogenous proliferation marker Ki-67 and for the preoperatively administered proliferation marker iododeoxyuridine. The sensitivity, specificity, positive predictive value, and negative predictive value were calculated for ^{18}F-FLT PET. **Results:** Primary tumor sites were oral cavity (n = 7), larynx (n = 2), and maxillary sinus (n = 1). Nine of the 10 patients examined had ^{18}F-FLT PET-positive lymph nodes (SUV_{mean}: median, 1.2; range, 0.8–2.9), but only 3 of these patients had histologically proven metastases. All metastatic lymph nodes showed Ki-67 and iododeoxyuridine staining in tumor cells. In the remaining 7 patients, there was abundant Ki-67 and iododeoxyuridine staining of B-lymphocytes in germinal centers in PET-positive lymph nodes, explaining the high rate of false-positive findings. The sensitivity, specificity, positive predictive value, and negative predictive value of ^{18}F-FLT PET were 100%, 16.7%, 37.5%, and 100%, respectively. **Conclusion:** In head and neck cancer patients, ^{18}F-FLT PET showed uptake in metastatic as well as in nonmetastatic reactive lymph nodes, the latter due to reactive B-lymphocyte proliferation. Because of the low specificity, ^{18}F-FLT PET is not suitable for assessment of pretreatment lymph node status. This observation may also negatively influence the utility of ^{18}F-FLT PET for early treatment response evaluation of small metastatic nodes.

Key Words: ^{18}F-FLT; PET/CT; staging; head and neck cancer

J Nucl Med 2007; 48:726–735
DOI: 10.2967/jnumed.106.037473

Lymph node involvement in squamous cell carcinoma of the head and neck is an indicator of poor prognosis, reducing the cure rate by almost 50% (*1*). Standard diagnostic work-up for assessing cervical lymph node status is performed by CT or MRI. The sensitivity (50%–80%) and specificity (70%–90%) of CT and MRI are comparable (*2,3*). For marginally enlarged lymph nodes, examination by ultrasound imaging (US) with fine-needle aspiration cytology is superior to CT and MRI if performed by an experienced radiologist (sensitivity and specificity up to 76% and 100%, respectively (*4,5*)). More recently, several studies have been performed to assess the value of ^{18}F-FDG PET for cervical lymph node staging (*6–11*). The results of these studies indicate that the performance of ^{18}F-FDG PET is not clearly superior to US, CT, or MRI. Therefore, ^{18}F-FDG PET is generally not considered as part of the standard work-up for head and neck cancer patients for this indication.

An additional biologic factor of prognostic relevance is tumor cell proliferation. Head and neck squamous cell carcinomas show accelerated repopulation of clonogenic tumor cells during the course of radiation therapy, and this is related to poor treatment outcome (*12–15*). Several treatment modifications have been developed to counteract this phenomenon, such as accelerated radiotherapy and inhibition of the epidermal growth factor receptor, but at the cost

Received Oct. 20, 2006; revision accepted Feb. 12, 2007.
For correspondence or reprints contact: Esther G.C. Troost, MD, Department of Radiation Oncology, Radboud University Nijmegen Medical Centre, P.O. Box 9101, 6500 HB Nijmegen, The Netherlands.
E-mail: e.troost@rther.umcn.nl
COPYRIGHT © 2007 by the Society of Nuclear Medicine, Inc.

of increased toxicity for the patient (*16–18*). Hence, careful patient selection for these treatment strategies is required to ensure maximal patient benefit and prevent undue toxicity and costs.

A diagnostic tool to identify lymph node metastases with high accuracy that can also provide information on the proliferative activity of the tumor could be of great value for treatment selection and radiotherapy planning.

Shields et al. introduced the novel PET tracer 3′-deoxy-3′-^{18}F-fluorothymidine (^{18}F-FLT) that is monophosphorylated by the cytosolic enzyme thymidine kinase 1 (TK1) and trapped intracellularly (*19*). TK1 activity is increased during DNA synthesis, and ^{18}F-FLT trapping is related to TK1 activity and thus to proliferation. It is of importance to note that ^{18}F-FLT is not incorporated into the DNA and that this TK1-mediated pathway could theoretically be upregulated, although DNA synthesis is inhibited. A number of studies evaluated the usefulness of ^{18}F-FLT in assessing tumor cell proliferation in the primary tumor, most of them including a comparison with ^{18}F-FDG PET (*20–31*). Several studies validated ^{18}F-FLT tracer uptake with the proliferation marker Ki-67 in primary tumor resection material or biopsies (*23,30–35*). A single study on laryngeal carcinoma by Cobben et al. compared ^{18}F-FLT with ^{18}F-FDG PET for imaging of the primary tumor without histologic verification (*27*). To our knowledge, only 3 studies—2 on breast carcinoma and 1 on thoracic tumors—have validated ^{18}F-FLT PET versus histopathology for the detection of metastatic lymph nodes (*20,30,31*).

Different markers have been used for histologic assessment of proliferation. These include endogenous markers—such as Ki-67, proliferating cell nuclear antigen (PCNA), and members of the cyclin group—or intravenous administration of the thymidine analogs bromodeoxyuridine (BrdUrd) and iododeoxyuridine (IdUrd) (*36–38*). The latter have a short half-life and are rapidly incorporated in the DNA of S-phase cells (*39*). For immunohistochemical validation of ^{18}F-FLT, these thymidine analogs seem most suitable because TK1 activity is increased primarily during DNA synthesis.

Thus far, validation of the PET tracer ^{18}F-FLT has focused mainly on primary tumor sites, and only recently was this expanded to determining lymph node status. Characterization of both the primary tumor and the lymph nodes is compulsory for selection of the treatment strategy in patients with squamous cell carcinomas of the head and neck. The aim of this study was to determine the value of ^{18}F-FLT PET for assessment of the cervical lymph node status and proliferative activity with histologic evaluation as the gold standard.

METHODS AND MATERIALS

Patients

Ten patients with newly diagnosed stage II–IV primary squamous cell carcinoma of the head and neck, awaiting surgical tumor and lymph node resection, were included in this study after giving written informed consent. The study was approved by the Institutional Review Board of the Radboud University Nijmegen Medical Centre, The Netherlands.

^{18}F-FLT Synthesis

^{18}F-FLT was obtained commercially from the Cyclotron B.V., VU Medical Centre, Amsterdam, The Netherlands. Synthesis was performed according to the method of Machulla et al. (*40*). In brief, ^{18}F-FLT was produced by ^{18}F-fluorination of the 4,4′-dimethoxytrityl−protected anhydrothymidine, followed by a deprotection step. After purification by reverse-phase high-performance liquid chromatography, the product was made isotonic and passed through a 0.22-μm filter. ^{18}F-FLT was produced with a nondecay-corrected radiochemical yield of 5%–10%, a radiochemical purity of >95%, and a specific activity of >10 TBq/mmol.

PET/CT Acquisition

Before surgical tumor resection, integrated PET and CT images were acquired either with a hybrid PET/CT system (patients 7, 9, and 10) or with software fusion of dedicated PET and CT images (all remaining patients). All scans were performed with the patient positioned in a rigid customized mask covering the head/neck area to increase position accuracy and to reduce movement artifacts during PET scanning.

Hybrid PET/CT images were acquired using a Biograph Duo scanner (Siemens Medical Solutions). Emission images of the head and neck area were recorded 60 min after intravenous injection of 250 MBq ^{18}F-FLT, with 7 min per bed position in 3-dimensional (3D) mode. PET images were reconstructed using the ordered-subset expectation maximization (OSEM) iterative algorithm with parameters optimized for the head and neck area (i.e., 4 iterations, 16 subsets, and 5-mm 3D gaussian filter), with correction for photon attenuation. In addition, CT images were acquired with 120 mA·s, 130 kV, and a slice width of 3 mm, with intravenous contrast in the venous phase, for anatomic correlation and attenuation correction purposes.

Dedicated PET images were acquired using an ECAT Exact scanner (Siemens Medical Solutions). Emission and transmission images of the head and neck area were recorded 60 min after intravenous injection of 250 MBq ^{18}F-FLT, with 5 min per bed position in 3D mode for emission and 3 min per bed position in 2-dimensional mode for transmission. PET image reconstruction was identical to that used for images from hybrid PET/CT. Dedicated CT images were acquired using a AcQsim CT scanner (Philips), with the same acquisition parameters as CT images from hybrid PET/CT. PET and CT image sets were anatomically coregistered using iterative-closest-point–based optimization of surface maps derived from PET transmission and CT images, with an average registration accuracy of 3 mm (*41*).

PET Analysis

Before analyzing the histologic sections, the combined PET/CT image sets were reviewed in consensus by 2 experienced observers who were unaware of all patient data. Images were scored for the presence or absence of ^{18}F-FLT PET uptake. Lymph node levels were determined as described by Gregoire et al. (*42*). Maximum and mean standardized uptake values (SUV_{max} and SUV_{mean}) were calculated for visible lymph nodes. SUV_{mean} was calculated after constructing a region of interest at the 50% isocontour of the SUV_{max}.

Surgery

Twenty minutes before the start of surgery, IdUrd (Centre Hospitalier Universitaire Vaudois, Lausanne, Switzerland), 200 mg diluted in 100 mL of 0.9% NaCl, was administered intravenously as a bolus injection. After resection, the neck dissection specimens were presented on a uniform left- or right-sided plate resembling the neck levels I–VI.

Immunohistochemical Staining of IdUrd and Ki-67

From the 10 patients, a total of 236 lymph nodes without metastases and 14 lymph nodes with metastatic involvement localized in 44 lymph node levels were removed. From these, paraffin blocks containing lymph nodes from 26 different lymph node levels were collected for this study. These included 18 ^{18}F-FLT PET-positive lymph node levels and 8 randomly chosen levels that were ^{18}F-FLT PET-negative.

From these blocks, 5-μm sections were cut and consecutive sections were stained for Ki-67 and IdUrd. Between all consecutive steps of the staining procedure, lymph node sections were rinsed with 0.1 M phosphate-buffered saline (Klinipath), pH 7.4. The staining procedures were performed at room temperature unless stated differently. The sections were deparaffinized and rehydrated in Histosafe (Adamas Instrumenten B.V.) and graded alcohols. For antigen retrieval, slides were heated (90°C) in 10 mM citrate buffer, pH 6.0, for 30 min. For the Ki-67 staining, sections were incubated with 5% normal donkey serum diluted in primary antibody diluent (PAD; Abcam) at 37°C for 30 min. Sections were incubated overnight with mouse antihuman-Ki67 (Zymed Laboratories), undiluted, at 4°C.

For the IdUrd staining, sections were incubated with 2N HCl for 30 min, followed by incubation with 0.1 M borax for 15 min and with 5% normal donkey serum diluted in PAD at 37°C for 30 min. Then, sections were incubated with mouse anti-IdUrd (Caltag Laboratories), diluted 1:3,000, for 60 min. In both staining procedures, peroxidase was blocked with 3% H_2O_2 in methanol for 10 min. Next, all sections were incubated with donkey antimouse-biotin (Jackson Immuno Research Laboratories), diluted 1:400, for 60 min and with ABC reagent (Vector Laboratories) for 30 min. Then, sections were rinsed with deionized water before incubation with diaminobenzidine (Zymed Laboratories) for 15 min. Finally, after rinsing with tap water and staining with hematoxylin (Klinipath) for 30 s, sections were dehydrated and covered with mounting medium (Klinipath) and a coverslip.

Pathology Evaluation and Assessment of Proliferation

The removed lymph nodes were routinely stained with hematoxylin and eosin (H&E) and assessed for metastatic involvement by a pathologist. Next, the clinical investigators and an experienced pathologist reviewed all lymph node sections stained for Ki-67 and IdUrd. On the basis of ^{18}F-FLT PET images and pathologic findings, lymph nodes were assigned to one of 4 groups: true-positive (^{18}F-FLT-positive lymph node with histologically proven metastasis), true-negative (^{18}F-FLT-negative lymph node without metastasis), and false-positive (^{18}F-FLT-positive lymph node without metastasis) or false-negative (^{18}F-FLT-negative lymph node with histologically proven metastasis).

Three histologically distinct areas were distinguished in the lymph node sections: germinal centers, metastatic tumor (if present), and the remaining lymphoid tissue. In these areas, Ki-67- and IdUrd-positive and negative nuclei were counted using a grid with 25 fields placed in the eyepiece at 200× magnification (3 randomly

TABLE 1
Patient Characteristics, Diagnostic and Therapeutic Procedures, and Histopathology of Lymph Nodes

Patient no.	Site	US and FNA cytology (side)	CT	MRI	Clinical stage	Pathologic stage	Procedure	Pathology LN (no. of Pathologic LN)		LN positive on PET* (no. of LN indicated)		LN positive on PET† (no. and side of LN indicated)
								L	R	L	R	
1	Maxillary sinus	POS (L)	NP	POS	T4N1M0	pT4pN1M0	TE + MRND, L	POS (1)	NA	1	NA	1, R
2	Laryngeal	NP	NEG	NP	T3N0M0	pT3pN0M0	TLE + bilateral NS	NEG	NEG	1	1	2, R
3	Laryngeal	NP	POS	NP	T4N2cM0	pT4pN2cM0	TLE + bilateral RND	POS (7)	POS (5)	2	2	1, R
4	Lower alveolar ridge	NEG (L)	NEG	NP	T4N2bM0	pT4pN0M0	TE + MRND, R	NA	NEG	NA	2	2, L
5	Floor of mouth	NR	NP	NP	T2N0M0	pT2pN0M0	TE + bilateral SND	NEG	NEG	NEG	NEG	—
6	Tongue	NEG (R)	NP	NP	T3N0M0	pT2pN0M0	TE + SND, R	NA	NEG	—	5	—
7	Soft palate	NP	NP	NP	T2N0M0	pT2pN0M0	TE + SND, L	NEG	NA	NEG	NA	1, R
8	Tongue	NP	NP	NEG	T3N0M0	pT3pN1M0	TE + SND, R	NA	POS (1)	—	1	1, R
9	Tongue/floor of mouth	NEG (L)	NP	NEG	T4N0M0	pT2pN0M0	TE + SND, L	NEG	NA	3	NA	2, R
10	Tongue/floor of mouth	NEG (L)	NP	NEG	T2N0M0	pT2pN0M0	TE + SND, L	NEG	NA	2	—	—

*Available for pathologic assessment.
†Not available for pathologic assessment.
LN = lymph node; FNA = fine-needle aspiration; NP = not performed; POS = positive; TE = tumor excision; MRND = modified radical neck dissection; NA = not available; NEG = negative; TLE = total laryngectomy; NS = node sampling; RND = radical neck dissection; NR = not representative; SND = selective neck dissection (level I–III).

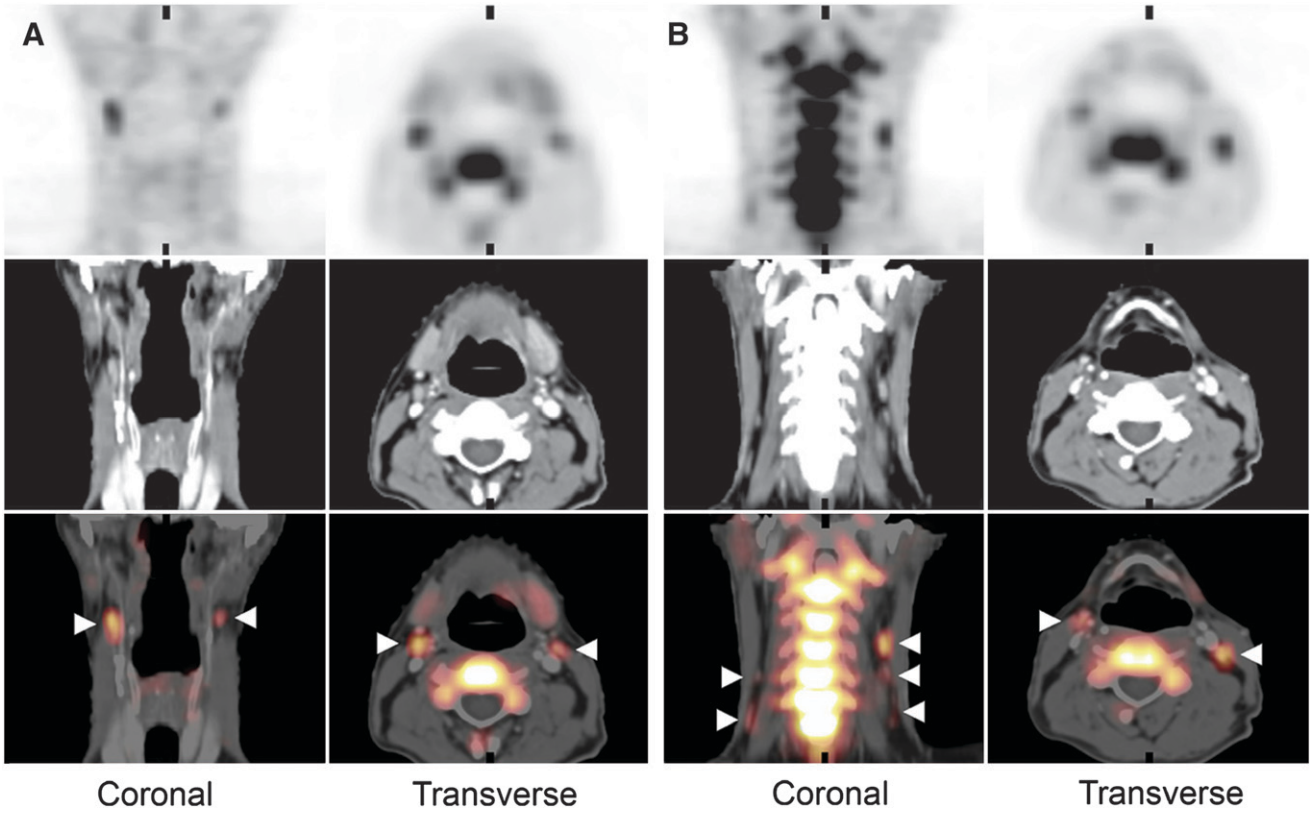

FIGURE 1. ^{18}F-FLT PET/CT images of patient 9 (pT2pN0M0 oral cavity carcinoma). Top panels show PET images, middle panels show CT images, and bottom panels show fusion of both image modalities. Cervical lymph nodes with increased ^{18}F-FLT uptake are found bilaterally in level II (A, arrowheads) and in levels III and IV (B, arrowheads). All lymph nodes detected with ^{18}F-FLT in this example were false-positive for metastasis, due to uptake in proliferating B-lymphocytes in reactive germinal centers.

selected fields were analyzed in germinal centers, 3 fields in metastatic tissue, and 1 field in the remaining lymphoid tissue). The Ki-67 and IdUrd labeling index (LI) was determined as the number of positively stained nuclei relative to the total number of nuclei in a certain area.

The total lymph node area and the (relative) area occupied by germinal centers—and, if present, metastatic tumor—were calculated in all lymph node sections. This was done by scanning the entire section under bright-field microscopy and reconstructing a composite image of the complete lymph node using image analysis software (IPLab; Scanalytics Inc.). Masks were drawn on these scans, indicating the total lymph node area, the germinal centers, and metastatic tumor deposits. Next, using the image analysis software, the absolute and relative areas occupied by germinal centers and metastatic deposits were calculated.

SUV_{mean} Versus Ki-67 and IdUrd Staining

As a measure of total proliferative activity in the germinal centers of a lymph node section, the product of the Ki-67 or IdUrd LI and the absolute area occupied by the germinal centers was calculated. These parameters were termed $Ki\text{-}67_{germinal\ center}$ and $IdUrd_{germinal\ center}$. Similarly, as a measure of total proliferative activity in the entire lymph node, the sum of the products of LI and absolute area of germinal centers and remaining lymphoid tissue—and, if present, metastatic deposits—was calculated; these were termed $Ki\text{-}67_{lymph\ node}$ and $IdUrd_{lymph\ node}$. These parameters were compared between true-positive, false-positive, and true-negative lymph nodes and were correlated with SUV_{mean}.

Statistical Analysis

The ANOVA test was used to assess differences in absolute area and Ki-67 and IdUrd LI between true-negative, false-positive, and true-positive lymph nodes. The *t* test was applied for comparison of number and absolute area of germinal centers and for comparison of $Ki\text{-}67_{germinal\ center}$ and $IdUrd_{germinal\ center}$ between true-negative and false-positive lymph nodes. Correlations between $Ki\text{-}67_{lymph\ node}$ and $IdUrd_{lymph\ node}$ and SUV_{mean} were calculated using linear regression. All statistical analyses were calculated using GraphPad Prism (version 4.0a). $P \leq 0.05$ was regarded as statistically significant.

RESULTS

Patients and Treatment

Patient characteristics are summarized in Table 1. Four men and 6 women with a mean age of 59 y (range, 43–80 y) were included. Primary tumor sites were oral cavity ($n = 7$), larynx ($n = 2$), and maxillary sinus ($n = 1$). Preoperative staging of the neck was performed with US (8 patients)—with fine-needle aspiration cytology in 6 patients and without in 2 patients—with CT (3 patients), or with MRI (4 patients). All patients underwent surgical tumor resection combined with assessment of cervical lymph node involvement according to

TABLE 2
Histologic Lymph Node Assessment: SUV_{mean}, Histopathology, and Mean Ki-67 and IdUrd Staining

Patient no.	LN level			Pathology		Ki-67 and IdUrd staining		
	^{18}F-FLT POS	SUV_{mean}	^{18}F-FLT NEG	Metastasis	Group	Metastasis	Germinal centers	Remaining LN tissue
1	R II	1.5		NA				
			L III	−	TN	−	+	+
	L II	2.9		+	TP	+	−	+
2	R II	1.2		−	FP	−	++	+
	R III	0.9		NA				
	R IV	1.2		NA				
	L III	1.1		−	FP	−	++	+
3	R II	1.2		NA				
	R III	1.3		+	TP	+	++	+
	R IV	1.1		+	TP	+	++	+
	L II	1.7		+	TP	+	−	−
	L IV	1.3		+	TP	+	+	+
4	R II	1.4		−	FP	−	++	+
			R III	−	TN	−	−	+
	R IV	1.1		−	FP	−	−	+
			R V	−	TN	−	++	+
	L II	1.0		NA				
	L IV	0.8		NA				
5			R I	−	TN	−	+	+
			L II	−	TN	−	+	++
6	R I	1.4		−	FP	−	++	++
	R II	1.3		−	FP	−	++	++
	R III	0.9		−	FP	−	+	+
7	R IV	1.5		NA				
			L I	−	TN	−	++	+
			L III	−	TN	−	++	+
8	R II	1.0		+	TP	+	++	+
	R III	0.8		NA				
9	R II	2.1		NA				
	R IV	1.0		NA				
	L II	1.3		−	FP	−	++	+
	L III	2.0		−	FP	−	+	+
	L IV	1.0		−	FP	−	+	+
			L I	−	TN	−	−	+
10	L II	1.6		−	FP	−	+	++
	L III	1.3		−	FP	−	+	++

LN = lymph node; POS = positive; NEG = negative; II = level indicated by roman number, NA = not available; TN = true-negative ^{18}F-FLT-negative lymph node without metastasis; TP = true-positive ^{18}F-FLT-positive lymph node with metastasis; FP = false-positive ^{18}F-FLT-positive lymph node without metastasis.

Dutch National Guidelines: Six patients with clinically N0 oral cavity carcinoma underwent selective neck dissection of level I–III. A (modified) radical neck dissection was done in 3 patients with preoperatively proven cervical lymph node involvement. In 1 patient with a glottic laryngeal carcinoma without suspected lymph node involvement, only sampling of level II and III nodes was performed. Neck surgery was performed unilaterally in 7 patients and bilaterally in 3 patients.

^{18}F-FLT PET

^{18}F-FLT PET scans were acquired simultaneously on PET/CT ($n = 3$) or consecutively on CT and PET ($n = 7$). The median time interval between ^{18}F-FLT PET and surgery was 5 d (average, 9.9 d; range, 4–37 d). In all but one case, surgery was performed within 4–14 d after the PET scan. In the case with the longest interval (37 d), the surgical resection of an oral cavity carcinoma was postponed because the patient underwent laser evaporation of a small laryngeal lesion first. In all but 1 patient (patient 5), increased mean SUVs ranging from 0.8 to 2.9 (median, 1.2; SD, 0.41) were detected, mostly in multiple lymph nodes. A typical ^{18}F-FLT PET/CT image is shown in Figure 1.

Pathologic Evaluation

Routine pathology based on H&E staining revealed 3 patients to have metastatic cervical lymph node disease (patients 1, 3, and 8), whereas clinical examination and

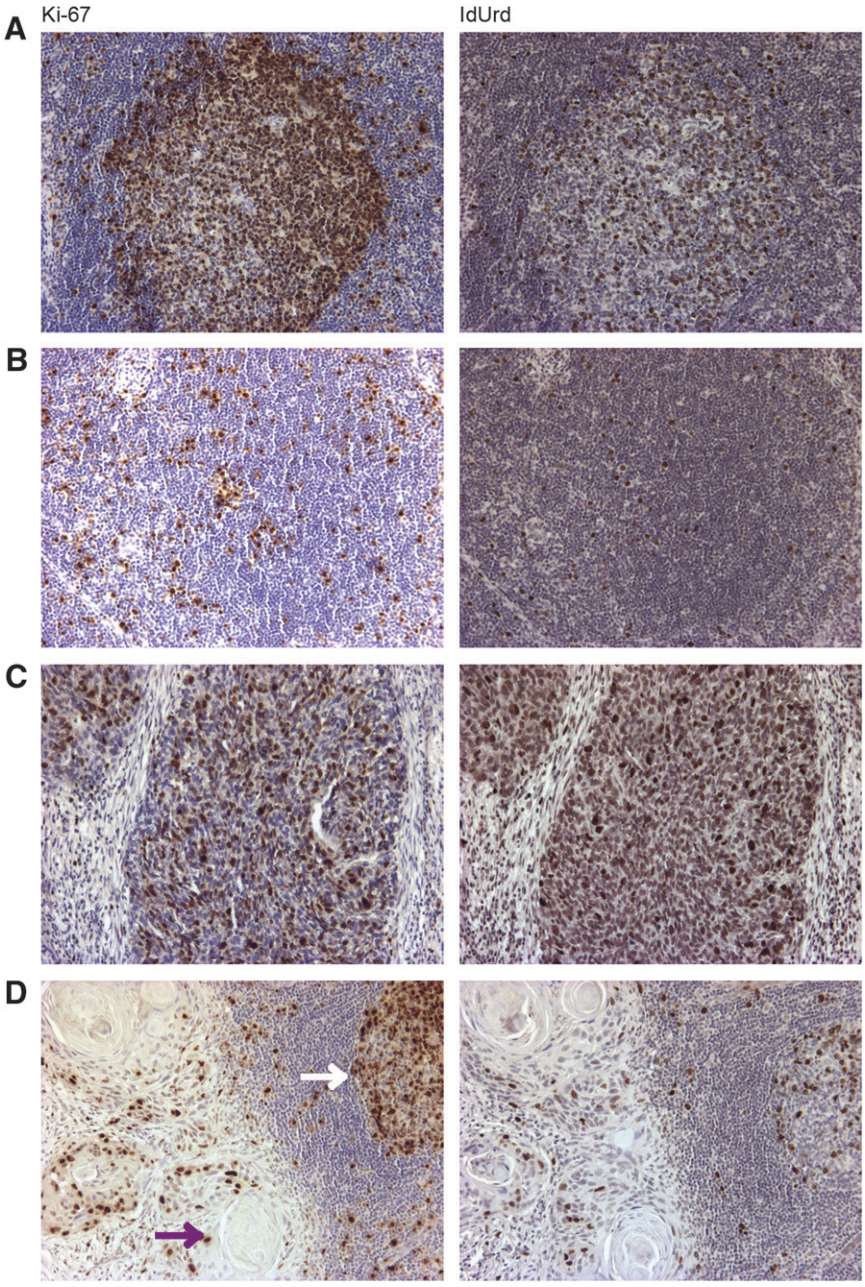

FIGURE 2. Ki-67 and IdUrd staining. (A) Germinal center harboring proliferating B-lymphocytes and remaining lymphoid tissue. (B) Remaining lymphoid tissue with proliferating lymphoid cells. (C) Metastasis of squamous cell carcinoma of maxillary sinus. (D) Micrometastasis with keratinization (purple arrow), fragment of a germinal center (white arrow), and surrounding lymphoid tissue. (×100)

anatomic imaging had predicted this finding only in 2 patients (patients 1 and 3). The third patient had a micrometastasis of <2 mm in 1 lymph node (patient 8). Although preoperative staging of the neck revealed multiple ipsilateral enlarged lymph nodes in patient 4, final histology showed no signs of metastatic disease.

In total, paraffin-embedded sections containing 26 lymph node levels were selected for Ki-67 and IdUrd staining and analysis. Eighteen of these levels were positive on ^{18}F-FLT PET, and 8 levels were negative. As shown in Table 2, comparison of ^{18}F-FLT PET results with pathology revealed 6 true-positive, 12 false-positive, and 8 true-negative findings. There were no false-negative ^{18}F-FLT PET studies. On the basis of these findings, the sensitivity of ^{18}F-FLT for determining lymph node status in head and neck cancer patients was 100%, the specificity was 40%, the positive predictive value was 33.3%, and the negative predictive value was 100% on the lymph node level. On the patient level, after excluding patient 7—as no histologic correlate for the ^{18}F-FLT-positive lymph node was available—the values were 100%, 16.7%, 37.5%, and 100%, respectively.

Not all lymph nodes showing enhanced ^{18}F-FLT PET uptake were removed during surgery. These lymph nodes were not included in the neck dissection specimen (patients 3 and 8) or were situated in the contralateral neck (patients 1, 2, 4, 7, and 9). On the basis of the results of the standard diagnostic work-up and therapeutic guidelines, there was no indication for removal of these nodes.

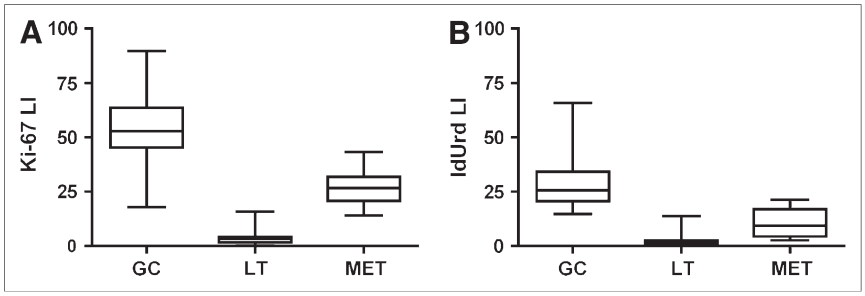

FIGURE 3. Ki-67 LI (A) and IdUrd LI (B) in germinal centers (GC), remaining lymphoid tissue (LT), and metastases (MET).

Follow-up (median, 13 mo; range, 11–15 mo) revealed recurrent primary tumor in 1 patient treated with surgery and postoperative radiotherapy (pT2pN0M0 carcinoma of the tongue). Until present, no lymph node recurrence has been observed in any of the patients.

Ki-67 and IdUrd Staining

Ki-67 and IdUrd staining was present in metastatic tumor cells, germinal centers, and in remaining lymphoid tissue as shown in Figure 2. In almost all lymph nodes examined—both ^{18}F-FLT PET-positive and -negative—germinal centers staining positive for Ki-67 and IdUrd were present. Metastatic tumor cells in patients 1 and 3 had almost fully destroyed the lymph node architecture. In patient 8, the micrometastasis occupied only a small region of the affected lymph node, leaving reactive germinal centers and remaining lymph node tissue unperturbed.

In germinal centers, metastases, and remaining lymphoid tissue, nuclei staining positive for Ki-67 and IdUrd were counted and the LI was calculated. Figure 3 shows the overall results for Ki-67 LI and IdUrd LI in these 3 lymph node areas. Table 3 presents the quantitative data for Ki-67 LI and IdUrd LI in the germinal centers, remaining lymphoid tissue, metastases and overall for the true-negative, false-positive, and true-positive lymph nodes. The median Ki-67 LI and IdUrd LI in the germinal centers were 52.8% and 25.7%, respectively, with no difference between the 3 groups. In the remaining lymphoid tissue, the median Ki-67 LI and IdUrd LI were 3.3% and 1.6%, respectively, also with no difference between the groups. In the metastases, the median LI was 26.7% for Ki-67 and 9.3% for IdUrd. In all 3 areas and patient groups studied, Ki-67 LI was significantly higher compared with IdUrd LI ($P < 0.0001$).

Germinal Centers

The median number of germinal centers per lymph node was 9 (SD, 6.7) in true-negative lymph nodes, 20.5 (SD, 27.0) in false-positive nodes, and 4 (SD, 18.1) in true-positive nodes. The difference in number of germinal centers between true-negative and false-positive lymph nodes was significant ($P = 0.03$). Also, the absolute area occupied by germinal centers was higher in false-positive nodes relative to true-negative nodes, but the difference was only borderline significant ($P = 0.06$) (Fig. 4A). The total proliferative activity in the germinal centers expressed as $\text{Ki-67}_{\text{germinal center}}$ and $\text{IdUrd}_{\text{germinal center}}$ was higher in the false-positive lymph nodes compared with the true-negative nodes, although the difference did not reach statistical significance ($P = 0.07$, respectively) (Figs. 4B and 4C).

TABLE 3
Ki-67 LI and IdUrd LI in Germinal Centers, Remaining Lymphoid Tissue, and Metastases

Ki-67 LI									
	Germinal centers				Remaining lymphoid tissue				Metastases
Parameter	TN	FP	TP	Overall	TN	FP	TP	Overall	TP
Mean	58.6	52.1	50.5	53.9	3.7	2.8	7.4	3.8	26.8
SD	16.6	13.2	4.2	13.8	1.9	2.4	7.5	3.6	7.7
Median	55.1	53.1	49.5	52.8	3.6	2.5	4.6	3.3	26.7
IdUrd LI									
	Germinal centers				Remaining lymphoid tissue				Metastases
Parameter	TN	FP	TP	Overall	TN	FP	TP	Overall	TP
Mean	33.5	27.4	23.0	28.8	1.4	1.8	4.2	2.1	10.4
SD	15.7	9.4	4.5	11.7	0.7	1.3	6.4	2.8	6.1
Median	29.6	23.9	24.9	25.7	1.6	1.6	1.5	1.6	9.3

TN = true-negative (^{18}F-FLT-negative lymph node without metastasis); FP = false-positive (^{18}F-FLT-positive lymph node without metastasis); TP = true-positive (^{18}F-FLT positive lymph node with metastasis).

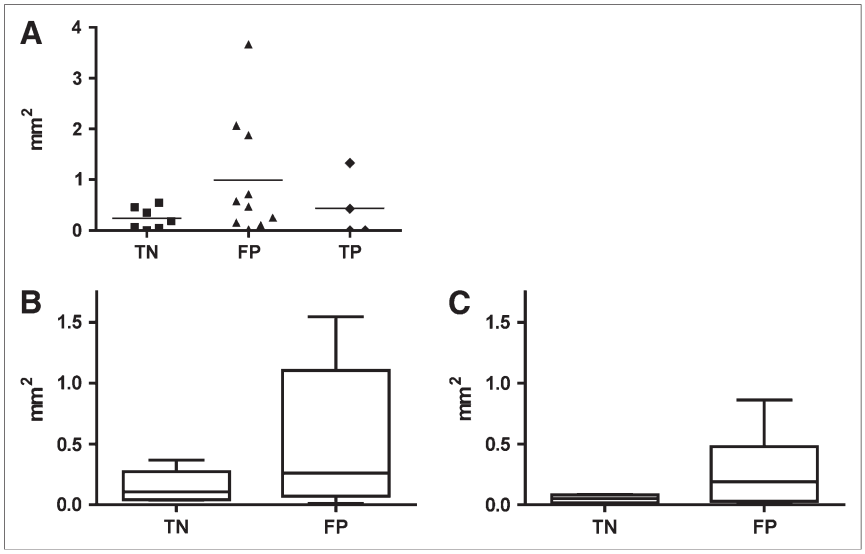

FIGURE 4. (A) Absolute area (in mm^2) occupied by germinal centers in true-negative (TN; ^{18}F-FLT-negative lymph node without metastasis), false-positive (FP; ^{18}F-FLT-positive lymph node without metastasis), and true-positive (TP; ^{18}F-FLT-positive lymph node with metastasis) lymph nodes. Ki-$67_{germinal\ center}$ (B) and $IdUrd_{germinal\ center}$ (C) in TN and FP lymph nodes as measure of total proliferative activity in germinal centers (calculated as area in mm^2).

Total Proliferative Activity in Lymph Nodes and Correlation with SUV_{mean}

The total proliferative activity in lymph nodes expressed as Ki-$67_{lymph\ node}$ and $IdUrd_{lymph\ node}$ was found to be significantly higher in the true-positive lymph nodes compared with that of false-positive lymph nodes ($P = 0.006$ and $P = 0.05$, respectively). As shown in Figure 5, there was a moderate but significant correlation between SUV_{mean} and Ki-$67_{lymph\ node}$ ($r^2 = 0.47$, $P = 0.0009$) and between SUV_{mean} and $IdUrd_{lymph\ node}$ ($r^2 = 0.55$, $P = 0.0004$).

DISCUSSION

The PET tracer ^{18}F-FLT has been studied for imaging of cell proliferation by various groups, correlating ^{18}F-FLT with ^{18}F-FDG (*20–31*). Buck et al. studied ^{18}F-FLT PET and ^{18}F-FDG PET in 47 patients with benign and malignant pulmonary nodules and found a high sensitivity of ^{18}F-FLT for malignant primary tumors (sensitivity, 90%) but not for mediastinal lymph node involvement (sensitivity, 53%) or detection of lung metastasis (sensitivity, 67%) (*22*). Cobben et al. studied 21 patients with primary or recurrent laryngeal carcinomas (*27*). Data on the sensitivity and specificity for detection of the primary tumor were reported only for ^{18}F-FDG and not for ^{18}F-FLT. However, the SUV for ^{18}F-FLT was found to be significantly lower compared with the SUV for ^{18}F-FDG and therefore, the routine use of ^{18}F-FLT PET for detection of laryngeal carcinoma was not recommended (*27*). Additional studies correlated ^{18}F-FLT with histologic assessment of proliferation by Ki-67 labeling in fibrosarcoma, breast cancer, and lung cancer (*23,30–35*). In lung carcinoma, Buck et al. found that the Ki-67 LI correlated with ^{18}F-FLT uptake (*23*). This finding has recently been confirmed by Yap et al. (*31*). In a fibrosarcoma xenograft, Leyton et al. found that the ^{18}F-FLT uptake and PCNA LI were linearly correlated (*33*). In contrast to these studies, Smyczek-Gargya et al. found no correlation between the Ki-67 LI and ^{18}F-FLT uptake in primary breast carcinoma (*30*). Although the results are not entirely consistent, these studies suggest that ^{18}F-FLT PET may be of value for the quantification of tumor cell proliferation.

The value of ^{18}F-FLT PET in assessing the cervical lymph node status and proliferative activity of metastatic lymph nodes in squamous cell carcinoma of the head and neck was investigated in the current study. The endogenous proliferation marker Ki-67—which is expressed in the G1, S, G2, and M phase of the cell cycle—was chosen for comparison with ^{18}F-FLT PET, because endogenous markers do not require intravenous administration and because recent studies validated ^{18}F-FLT PET with Ki-67 (*23,30,31*). In addition, the exogenous marker IdUrd was used. IdUrd is a robust and specific S-phase marker, and it was hypothesized that this marker might correlate better with ^{18}F-FLT uptake, because TK1 activity is increased

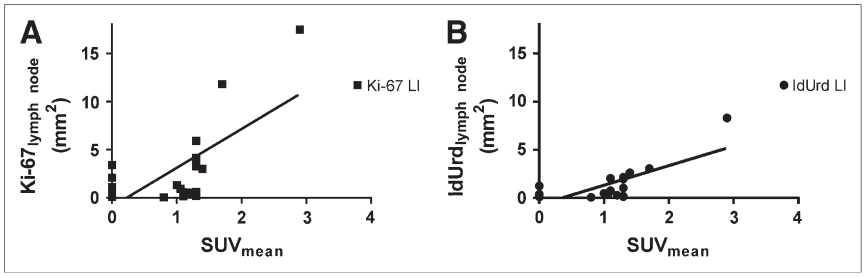

FIGURE 5. Scatter plot of Ki-$67_{lymph\ node}$ (A) and scatter plot of $IdUrd_{lymph\ node}$ (B) as measure of total proliferative activity in lymph node (calculated as area in mm^2) versus SUV_{mean} of ^{18}F-FLT PET. Solid lines indicate linear best fit.

mainly during DNA synthesis. In 9 of the 10 patients studied, increased ^{18}F-FLT uptake was observed in the lymph nodes. Only 3 of these 9 ^{18}F-FLT PET-positive patients had metastatic nodal disease confirmed by histopathology, and 2 of them had already been detected by routine preoperative screening. In none of the ^{18}F-FLT PET-negative lymph nodes was metastatic disease present.

As the number of false-positive lymph nodes was high, further analysis was performed taking into account the architecture and proliferative state of the lymph nodes. In most lymph nodes evaluated, intense staining of both Ki-67 and IdUrd was present in B-lymphocytes proliferating in germinal centers. Less intense staining was found in metastatic tumor cell deposits, and the proliferative activity in the remaining lymph node tissue was very low. In germinal centers, the LI of both markers was significantly higher compared with that of metastases or lymphoid tissue. There was no difference in the proliferative activity in germinal centers between true-negative and false-positive lymph nodes. However, false-positive nodes, on average, contained a significantly greater number of germinal centers, and these occupied a larger absolute area relative to the true-negative nodes, although the statistical significance of this latter finding was only borderline. Also, the product of the Ki-67 LI and IdUrd LI and area occupied by germinal centers was higher in the false-positive lymph nodes compared with the true-negative lymph nodes. Therefore, it is likely that the active proliferation of B-lymphocytes in germinal centers is responsible for the false-positive ^{18}F-FLT PET results. This high proliferative activity of B-lymphocytes might also be responsible for the ^{18}F-FLT PET positivity of the micrometastasis in patient 8.

Three other studies, 2 in breast cancer and 1 in thoracic tumors, compared ^{18}F-FLT PET with histopathology for the assessment of lymph node status (*20,30,31*). The study by Smyczek-Gargya et al. included 14 breast cancer patients, of whom 8 had histologically proven axillary lymph node metastasis and 7 were detected by ^{18}F-FLT PET (sensitivity, 87.5%; specificity, 100%) (*30*). In the study by Been et al. that included 10 patients, only 2 of 7 patients with histologically proven metastatic axillary lymph nodes were detected by ^{18}F-FLT PET (sensitivity, 28.5%; specificity, 100%) (*20*). Yap et al. studied 22 patients with thoracic tumors and reported the sensitivity and specificity for detection of mediastinal lymph nodes by ^{18}F-FLT to be 33.3% and 98.2%, respectively (*31*). The low sensitivity in some of these studies may be explained by the fact that some histologic tumor types, such as mammary carcinoma, can exhibit limited proliferative activity. A second explanation might be that the metastatic tumor load of some of these lymph nodes was low.

All 3 studies reported a high specificity in contrast to the current study, in which the specificity was only 16.7%. The localization of the lymph nodes may be of importance in explaining this discrepancy. Reactive lymph nodes in the head and neck area are found frequently as a response to bacterial or viral infections, whereas reactive axillary lymph nodes are less common. Furthermore, patients with squamous cell carcinomas of the oral cavity—the largest patient group in this study—often present with nonhealing ulcers accompanied by reactive lymph nodes. This is consistent with the observation that false-positive lymph nodes, on average, contained a higher subvolume of germinal centers with very active proliferation of B-lymphocytes as compared with true-negative nodes.

In this study, ^{18}F-FLT PET reached only a low SUV_{mean} in metastatic as well as nonmetastatic cervical lymph nodes compared with the SUV for ^{18}F-FDG PET generally reported in head and neck cancer (*6–9*). This is in agreement with the previous finding for primary laryngeal tumors by Cobben et al. (*27*). In accordance with studies discussed, a significant correlation between the SUV_{mean} and the overall Ki-67 and IdUrd staining ($Ki\text{-}67_{lymph\ node}$ and $IdUrd_{lymph\ node}$) was found in this study (Fig. 5) (*31,33*). The correlation was strongest for IdUrd, and we recommend this marker for future studies with ^{18}F-FLT that include histologic validation.

CONCLUSION

Although ^{18}F-FLT PET correctly identified all head and neck cancer patients with metastatic lymph nodes, the specificity and positive predictive value were low due to tracer uptake in germinal centers of lymph nodes. Therefore, the use of ^{18}F-FLT PET for assessing pretreatment lymph node status and for determining the proliferative activity of affected lymph nodes is not encouraged in head and neck cancer patients. This also limits the usefulness of ^{18}F-FLT PET for radiation therapy planning and possibly for early treatment response evaluation of small metastatic lymph nodes. The value of ^{18}F-FLT PET for assessment of the proliferative state of the primary head and neck tumor and the relevance for radiotherapy planning is a topic of current investigations.

ACKNOWLEDGMENTS

The authors thank the nuclear medicine technologists for their assistance and excellent patient care. This work was supported by a Junior Researcher Grant (2006-38) of the Radboud University Nijmegen Medical Centre and by European Community Grant EC FP6 funding (BIOCARE contract LSHC-CT-2004-505785).

REFERENCES

1. Brockstein B, Haraf DJ, Rademaker AW, et al. Patterns of failure, prognostic factors and survival in locoregionally advanced head and neck cancer treated with concomitant chemoradiotherapy: a 9-year, 337-patient, multi-institutional experience. *Ann Oncol.* 2004;15:1179–1186.
2. van den Brekel MW, Castelijns JA, Stel HV, Golding RP, Meyer CJ, Snow GB. Modern imaging techniques and ultrasound-guided aspiration cytology for the assessment of neck node metastases: a prospective comparative study. *Eur Arch Otorhinolaryngol.* 1993;250:11–17.
3. Wide JM, White DW, Woolgar JA, Brown JS, Vaughan ED, Lewis-Jones HG. Magnetic resonance imaging in the assessment of cervical nodal metastasis in oral squamous cell carcinoma. *Clin Radiol.* 1999;54:90–94.

4. Takes RP, Righi P, Meeuwis CA, et al. The value of ultrasound with ultrasound-guided fine-needle aspiration biopsy compared to computed tomography in the detection of regional metastases in the clinically negative neck. *Int J Radiat Oncol Biol Phys.* 1998;40:1027–1032.
5. van den Brekel MW, Castelijns JA, Stel HV, et al. Occult metastatic neck disease: detection with US and US-guided fine-needle aspiration cytology. *Radiology.* 1991;180:457–461.
6. Adams S, Baum RP, Stuckensen T, Bitter K, Hor G. Prospective comparison of ^{18}F-FDG PET with conventional imaging modalities (CT, MRI, US) in lymph node staging of head and neck cancer. *Eur J Nucl Med.* 1998;25:1255–1260.
7. Dammann F, Horger M, Mueller-Berg M, et al. Rational diagnosis of squamous cell carcinoma of the head and neck region: comparative evaluation of CT, MRI, and ^{18}FDG PET. *AJR.* 2005;184:1326–1331.
8. Ng SH, Yen TC, Liao CT, et al. ^{18}F-FDG PET and CT/MRI in oral cavity squamous cell carcinoma: a prospective study of 124 patients with histologic correlation. *J Nucl Med.* 2005;46:1136–1143.
9. Stuckensen T, Kovacs AF, Adams S, Baum RP. Staging of the neck in patients with oral cavity squamous cell carcinomas: a prospective comparison of PET, ultrasound, CT and MRI. *J Craniomaxillofac Surg.* 2000;28:319–324.
10. Ng SH, Yen TC, Chang JT, et al. Prospective study of [^{18}F]fluorodeoxyglucose positron emission tomography and computed tomography and magnetic resonance imaging in oral cavity squamous cell carcinoma with palpably negative neck. *J Clin Oncol.* 2006;24:4371–4376.
11. Wensing BM, Vogel WV, Marres HA, et al. FDG-PET in the clinically negative neck in oral squamous cell carcinoma. *Laryngoscope.* 2006;116:809–813.
12. Kim JJ, Tannock IF. Repopulation of cancer cells during therapy: an important cause of treatment failure. *Nat Rev Cancer.* 2005;5:516–525.
13. Petersen C, Zips D, Krause M, et al. Repopulation of FaDu human squamous cell carcinoma during fractionated radiotherapy correlates with reoxygenation. *Int J Radiat Oncol Biol Phys.* 2001;51:483–493.
14. Taylor JM, Withers HR, Mendenhall WM. Dose-time considerations of head and neck squamous cell carcinomas treated with irradiation. *Radiother Oncol.* 1990; 17:95–102.
15. Withers HR, Taylor JM, Maciejewski B. The hazard of accelerated tumor clonogen repopulation during radiotherapy. *Acta Oncol.* 1988;27:131–146.
16. Kaanders JH, van der Kogel AJ, Ang KK. Altered fractionation: limited by mucosal reactions? *Radiother Oncol.* 1999;50:247–260.
17. Bonner JA, Harari PM, Giralt J, et al. Radiotherapy plus cetuximab for squamous-cell carcinoma of the head and neck. *N Engl J Med.* 2006;354:567–578.
18. Overgaard J, Hansen HS, Specht L, et al. Five compared with six fractions per week of conventional radiotherapy of squamous-cell carcinoma of head and neck: DAHANCA 6 and 7 randomised controlled trial. *Lancet.* 2003;362: 933–940.
19. Shields AF, Grierson JR, Dohmen BM, et al. Imaging proliferation in vivo with [F-18]FLT and positron emission tomography. *Nat Med.* 1998;4:1334–1336.
20. Been LB, Elsinga PH, de Vries J, et al. Positron emission tomography in patients with breast cancer using ^{18}F-3′-deoxy-3′-fluoro-l-thymidine (^{18}F-FLT): a pilot study. *Eur J Surg Oncol.* 2006;32:39–43.
21. Buck AK, Halter G, Schirrmeister H, et al. Imaging proliferation in lung tumors with PET: ^{18}F-FLT versus ^{18}F-FDG. *J Nucl Med.* 2003;44:1426–1431.
22. Buck AK, Hetzel M, Schirrmeister H, et al. Clinical relevance of imaging proliferative activity in lung nodules. *Eur J Nucl Med Mol Imaging.* 2005;32: 525–533.
23. Buck AK, Schirrmeister H, Hetzel M, et al. 3-Deoxy-3-[^{18}F]fluorothymidine-positron emission tomography for noninvasive assessment of proliferation in pulmonary nodules. *Cancer Res.* 2002;62:3331–3334.
24. Chen W, Cloughesy T, Kamdar N, et al. Imaging proliferation in brain tumors with ^{18}F-FLT PET: comparison with ^{18}F-FDG. *J Nucl Med.* 2005;46:945–952.
25. Choi SJ, Kim JS, Kim JH, et al. [^{18}F]3′-Deoxy-3′-fluorothymidine PET for the diagnosis and grading of brain tumors. *Eur J Nucl Med Mol Imaging.* 2005;32: 653–659.
26. Cobben DC, Koopal S, Tiebosch AT, et al. New diagnostic techniques in staging in the surgical treatment of cutaneous malignant melanoma. *Eur J Surg Oncol.* 2002;28:692–700.
27. Cobben DC, van der Laan BF, Maas B, et al. ^{18}F-FLT PET for visualization of laryngeal cancer: comparison with ^{18}F-FDG PET. *J Nucl Med.* 2004;45:226–231.
28. Dittmann H, Dohmen BM, Paulsen F, et al. [^{18}F]FLT PET for diagnosis and staging of thoracic tumours. *Eur J Nucl Med Mol Imaging.* 2003;30:1407–1412.
29. Francis DL, Freeman A, Visvikis D, et al. In vivo imaging of cellular proliferation in colorectal cancer using positron emission tomography. *Gut.* 2003;52:1602–1606.
30. Smyczek-Gargya B, Fersis N, Dittmann H, et al. PET with [^{18}F]fluorothymidine for imaging of primary breast cancer: a pilot study. *Eur J Nucl Med Mol Imaging.* 2004;31:720–724.
31. Yap CS, Czernin J, Fishbein MC, et al. Evaluation of thoracic tumors with ^{18}F-fluorothymidine and ^{18}F-fluorodeoxyglucose-positron emission tomography. *Chest.* 2006;129:393–401.
32. Kenny LM, Vigushin DM, Al-Nahhas A, et al. Quantification of cellular proliferation in tumor and normal tissues of patients with breast cancer by [^{18}F]fluorothymidine-positron emission tomography imaging: evaluation of analytical methods. *Cancer Res.* 2005;65:10104–10112.
33. Leyton J, Latigo JR, Perumal M, Dhaliwal H, He Q, Aboagye EO. Early detection of tumor response to chemotherapy by 3′-deoxy-3′-[^{18}F]fluorothymidine positron emission tomography: the effect of cisplatin on a fibrosarcoma tumor model in vivo. *Cancer Res.* 2005;65:4202–4210.
34. Muzi M, Vesselle H, Grierson JR, et al. Kinetic analysis of 3′-deoxy-3′-fluorothymidine PET studies: validation studies in patients with lung cancer. *J Nucl Med.* 2005;46:274–282.
35. Vesselle H, Grierson J, Muzi M, et al. In vivo validation of 3′deoxy-3′-[^{18}F]fluorothymidine ([^{18}F]FLT) as a proliferation imaging tracer in humans: correlation of [^{18}F]FLT uptake by positron emission tomography with Ki-67 immunohistochemistry and flow cytometry in human lung tumors. *Clin Cancer Res.* 2002;8:3315–3323.
36. Begg AC, Haustermans K, Hart AA, et al. The value of pretreatment cell kinetic parameters as predictors for radiotherapy outcome in head and neck cancer: a multicenter analysis. *Radiother Oncol.* 1999;50:13–23.
37. Brown DC, Gatter KC. Ki67 protein: the immaculate deception? *Histopathology.* 2002;40:2–11.
38. Kelman Z. PCNA: structure, functions and interactions. *Oncogene.* 1997;14: 629–640.
39. Hughes WL, Commerford SL, Gitlin D, et al. Deoxyribonucleic acid metabolism in vivo. I. Cell proliferation and death as measured by incorporation and elimination of iododeoxyuridine. *Fed Proc.* 1964;23:640–648.
40. Machulla HJ, Blocher A, Kuntzsch M, Piert M, Wei R, Grierson JR. Simplified labeling approach for synthesizing 3′-deoxy-3′-[^{18}F]-fluorothymidine ([^{18}F]FLT). *J Radioanal Nucl Chem.* 2000;243:843–846.
41. Vogel WV, Schinagl DAX, van Dalen JA, Kaanders JHAM, Oyen WJG. Validated image fusion of dedicated PET and CT, for external beam radiation therapy in the head and neck area. *Q J Nucl Med.* In press.
42. Gregoire V, Coche E, Cosnard G, Hamoir M, Reychler H. Selection and delineation of lymph node target volumes in head and neck conformal radiotherapy: proposal for standardizing terminology and procedure based on the surgical experience tables. *Radiother Oncol.* 2000;56:135–150.